Charge-Transfer Complexes of a Conjugated Oligomer with Iodine: Evidence for Polaron, Bipolaron, and Ionized Bipolaron Formation

I. M. Brown*

McDonnell Douglas Research Laboratories, St. Louis, Missouri 63166

J. M. Wilbur

Chemistry Department, Southwest Missouri State University, Springfield, Missouri 65804.

Received July 23, 1987

ABSTRACT: This paper describes the results of electron spin resonance experiments on the charge-transfer complexes that are formed when the conjugated oligomer poly(4,4′-dibromobiphenyl-*co*-1,4-diethynylbenzene) is doped with iodine. The dependence of the spin susceptibility on the iodine content is interpreted in terms of the formation of polarons (radical cations with $S = {}^1/_2$), bipolarons (cations with $S = 0$), and ionized bipolarons (radical trications with $S = {}^1/_2$). The dependences of the effective g value and the line-shape parameters on the iodine content are explained in terms of an equilibria scheme involving different stoichiometric forms of these two types of radical cations. A dependence of the line-shape parameters on the radical concentration is also identified and is explained in terms of intermolecular spin–spin interactions.

Introduction

Many conjugated polymers exhibit high electrical conductivities when they are doped with electron acceptors such as iodine or arsenic pentafluoride.[1,2] In several of these studies, the magnetic properties that were determined by electron spin resonance spectroscopy (ESR) and related techniques have provided information that at best has led to a somewhat limited understanding of the conduction mechanisms in doped polymers. One feature difficult to understand is that in many cases the number of spins determined from the spin susceptibility is much less than the number of charge carriers.[3] To explain this discrepancy, Bredas et al.[4] have proposed the formation of spinless dication and dianion charge carriers called bipolarons. However, the existence of either charge carrier has been difficult to corroborate experimentally, primarily because of the diamagnetic nature of these bipolarons.

Our investigations described below involve a conjugated polymer that is in the form of a low-molecular-weight oligomer containing carbon–carbon triple bonds doped with iodine. Although such a system exhibits low electrical conductivity,[5] the ESR results provide some basic insight into the nature of the different types of species formed in conjugated polymers that have been doped with electron acceptors such as iodine. All these results are consistent with the formation of charge-transfer complexes in which the oligomer acts as the electron donor and iodine acts as the electron acceptor. As a result, radical cations form on the conjugated oligomer and charge compensation is brought about by the iodine anions. This paper presents evidence that polarons (radical cations), bipolarons (dications), and ionized bipolarons (radical trications) form in this oligomer sample at high iodine contents. The spin susceptibility and the ESR line-shape parameters show rather complicated dependences on the iodine content in the sample. These results are described below and are explained qualitatively in terms of the equilibria between different stoichiometric forms of these three species. At many iodine contents the radical concentrations are so high that electron spin–spin (both dipolar and exchange) interactions play an important role in determining the line shape parameters.

Experimental Section

The low-molecular-weight copolymer (oligomer) was prepared by the Pd(II)-catalyzed coupling reaction of 4,4′-dibromobiphenyl with 1,4-diethynylbenzene as illustrated in eq 1.

A high-molecular-weight polymer was not formed because the product oligomer precipitates from the reaction mixture, thus preventing further chain growth. Similar behavior has been observed in the Pd(II)-catalyzed copolymerization of other aromatic dihalides with various diethynylbenzenes.[6,7]

The IR spectrum and elemental analysis indicate that the oligomer is best represented by structure I. The absence of (C–H) stretching vibrations of the terminal –C≡CH group (3300 cm^{-1}) and the presence of the strong (C–H) bending vibrations of the *p*-phenylene and *p*-biphenylene groups (830–810 cm^{-1}), as well as the (C–Br) bending vibrations of the terminal Ar–Br group (1070 cm^{-1}) in the IR spectrum, suggest structure I. The bromine analysis provides additional evidence for this proposed structure. The theoretical value for the bromine content when the oligomer is terminated by two bromine atoms is 18.5 wt % which is in reasonable agreement with the experimental value of 17 wt %.

Iodine was added to the oligomer in the following manner. The sample was placed in a 4-mm tube inside a capped vial along with a few crystals of iodine. The vial was then heated in a temperature-controlled convection oven for times as short as 10 min and as long as 125 h at various temperatures from 365 to 390 K. After exposure to the iodine vapor, the yellow powder turned black. The iodine was removed from the sample by heating the sample tube in an empty uncapped vial in a vacuum oven at 375 K. The iodine content was determined from the increase in weight of the sample.

All the ESR spectra were obtained as first derivatives of the absorption by use of an X-band spectrometer (IBM Model 200D) interfaced to a computer (IBM 9001). The integrated ESR absorption intensities that were used as a measure of the spin susceptibilities were obtained from a double integration of the first-derivative spectra by use of the available software. The magnetic field values were determined with an NMR gaussmeter (Bruker Model ER-035M), and the microwave frequency was measured with a microwave frequency counter (EIP Model 575). The IR spectra of potassium bromide pellets containing the oligomer were obtained with a spectrophotometer (Perkin-Elmer Model 283). The triphenylphosphine, cuprous iodide, and palladium(II) acetate, were used in the as received condition. Elemental analyses were performed by Galbraith Laboratories, Knoxville, TN.

Copolymerization of 4,4′-Dibromobiphenyl and 1,4-Diethynylbenzene. The reaction flask, equipped with a mechanical stirrer, a reflux condenser, a calcium chloride drying tube, and a nitrogen inlet, was charged under nitrogen with 50 mL of dry toluene, 4,4′-dibromobiphenyl (3.12 g, 0.01 mol), freshly sublimed 1,4-diethynylbenzene (1.26 g, 0.01 mol), triphenylphosphine (507 mg, 1.93 mmol), cuprous iodide (73.6 mg, 0.39 mmol), palladium(II) acetate (21.7 mg, 0.097 mmol), and 20 mL of dry triethylamine. The reactants were heated at gentle reflux for 2.5 h under nitrogen with mechanical stirring. After cooling to room temperature, the reaction mixture was poured into 250 mL of

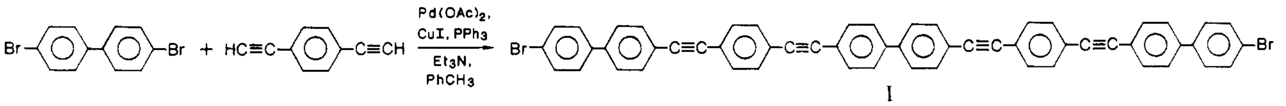

(1)

I

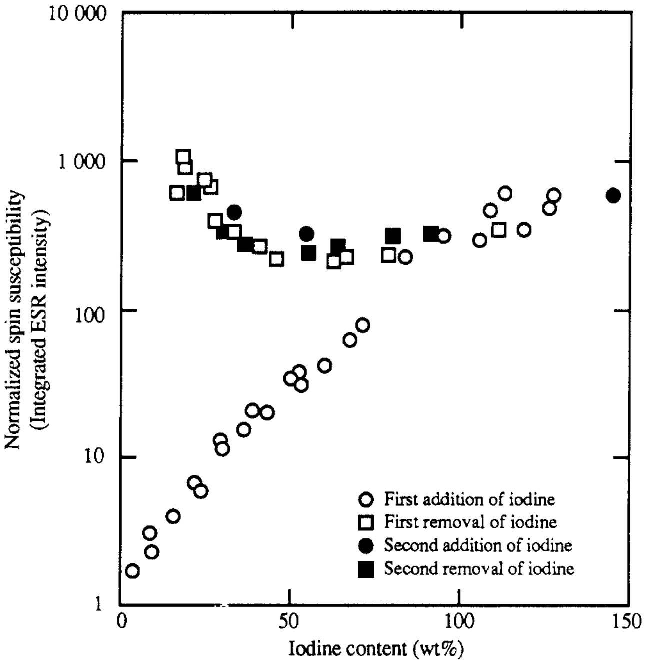

Figure 1. Spin susceptibility as a function of iodine content. The measured data were normalized to a value equal to 1.1 × the integrated intensity of the ESR absorption line observed in the samples before the addition of iodine.

methanol. The resulting yellow solid was collected by suction filtration and was washed successively with water, methanol, and ether and dried at room temperature under vacuum in a desiccator for 16 h. The yellow solid (2.58 g) was then purified by refluxing toluene over it for 16 h in a Soxhlet extractor. After the solid was dried under vacuum in a desiccator, 2.2 g (64.6%) of a toluene-insoluble yellow powder that did not melt below 360 °C was obtained and analyzed: IR (KBr) 1500, 1480, 1070, 830–810 cm^{-1}. Anal. Calcd for $C_{56}H_{32}Br_2$: C, 77.78; H, 3.73; Br, 18.48. Found: C, 77.56; H, 4.01; Br, 17.24.

Results and Discussion

It was evident from the color changes and the increase in the intensity of the ESR absorption that a chemical reaction had occurred after exposure of the oligomer sample to iodine vapor.

The spin susceptibility, effective g values, $\langle g \rangle$, and line shapes of the ESR spectra showed some reversible and some irreversible changes as iodine was both added and removed from the sample. The values of the spin susceptibility measured as a function of iodine content in the sample are shown in Figure 1. Since the spin susceptibility was determined from the integrated ESR intensity, these values can be considered a measure of the radical concentrations present. Figure 1 shows that on the first addition of iodine to the sample the radical concentration increases with increasing iodine content up to an iodine content ~120 wt %. On the other hand, when the iodine concentration is decreased, the radical concentration remains high, decreasing slightly at first and then increasing again below an iodine content of 50 wt %. As is also shown in Figure 1, the data obtained on the first removal, second addition, and second removal of iodine show that after the initial maximum doping, the measured values of spin susceptibility are reversible. We tentatively explain this surprising behavior in terms of the equilibria shown in Figure 2.

	Polaron states (S = 1/2)		Bipolaron states (s =0)		Ionized bipolaron states (S = 1/2)
$2P + 3I_2 \rightarrow$	$2P^{+}I_3^{-}$	$\overset{+3I_2}{\rightleftarrows}$	$2P^{+2}(I_3^{-})_2$	$\overset{+3I_2}{\rightleftarrows}$	$2P^{+3}(I_3^{-})_3$
	$\downarrow\uparrow + 2I_2$		$\downarrow\uparrow + 4I_2$		$\downarrow\uparrow + 6I_2$
	$2P^{+}I_5^{-}$	$\overset{+5I_2}{\rightleftarrows}$	$2P^{+2}(I_5^{-})_2$	$\overset{+3I_2}{\rightleftarrows}$	$2P^{+3}(I_5^{-})_3$

Figure 2. Proposed equilibria scheme.

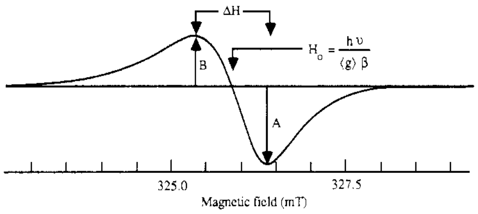

Figure 3. Definitions of $\langle g \rangle$, A/B, and ΔH.

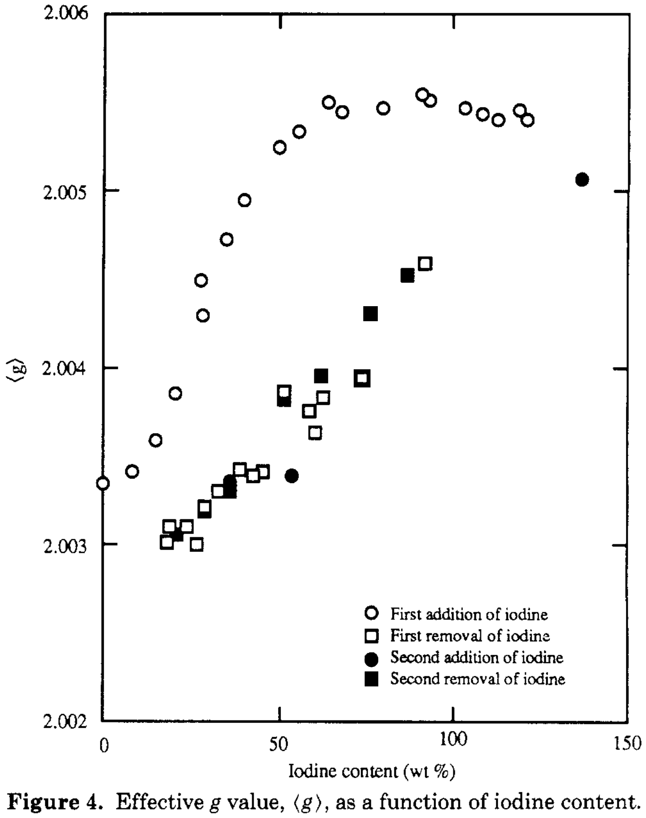

Figure 4. Effective g value, $\langle g \rangle$, as a function of iodine content.

For the equilibria scheme in Figure 2, we assume that three types of cations are formed: the singly charged cation which is paramagnetic ($S = {}^1/_2$), the doubly charged dication which is diamagnetic ($S = 0$), and the triply charged trication which is paramagnetic ($S = {}^1/_2$). In solid-state terminology, these species would correspond to a polaron, a bipolaron, and an ionized bipolaron, respectively. We have also included in this equilibria scheme the possibility that these cations can exist in different stoichiometric forms. The examples shown in Figure 2 include charge-compensating species such as I_3^- and I_5^-. These specific

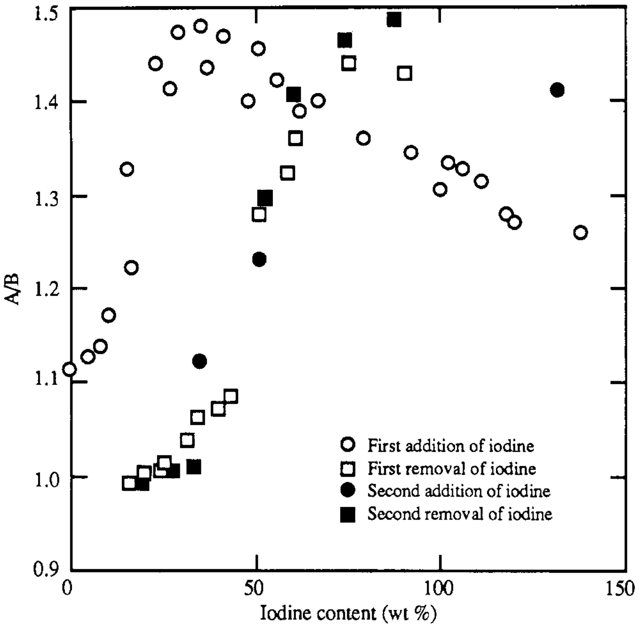

Figure 5. A/B ratio as a function of iodine content.

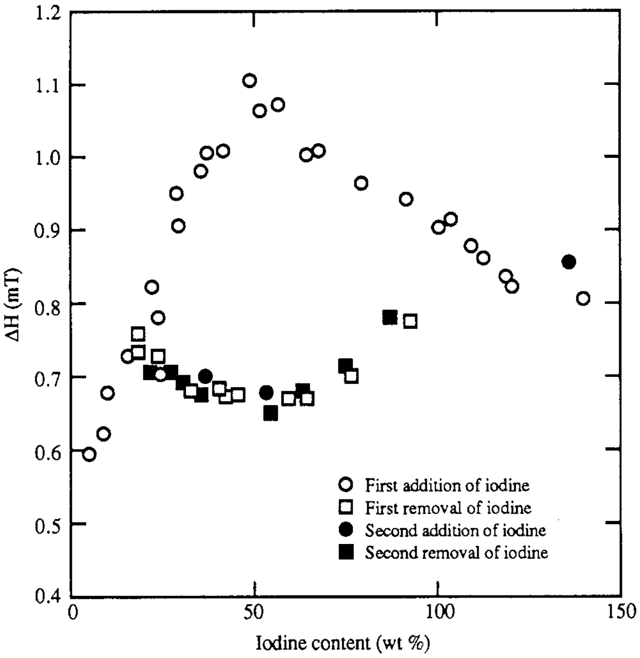

Figure 6. ΔH as a function of iodine content.

species are used for illustrative purposes to account for the changes in the line-shape parameters defined in Figure 3 and shown in Figures 4–6. In an actual sample there may be alternative or additional stoichiometric forms for the compensating species, e.g., $I_{(2n+1)}^-$ where $n \geq 1$.

According to the equilibria scheme in Figure 2, at high iodine concentrations (e.g., >100 wt %), all three types of cation will be present in their different stoichiometric forms. As the iodine concentration is reduced below 100 wt %, the equilibria will shift to the left, there will be a smaller relative amount of ionized bipolarons (paramagnetic), a larger number of bipolarons (diamagnetic), and the spin susceptibility will decrease. Moreover, below an iodine concentration of 50 wt %, the equilibria will move further to the left, the relative amounts of bipolarons will decrease, the amounts of polarons (paramagnetic) will increase, and hence the spin susceptibility will increase again. Thus, the equilibria scheme shown in Figure 2 can explain the behavior of the spin susceptibility, including the reversibility shown in Figure 1.

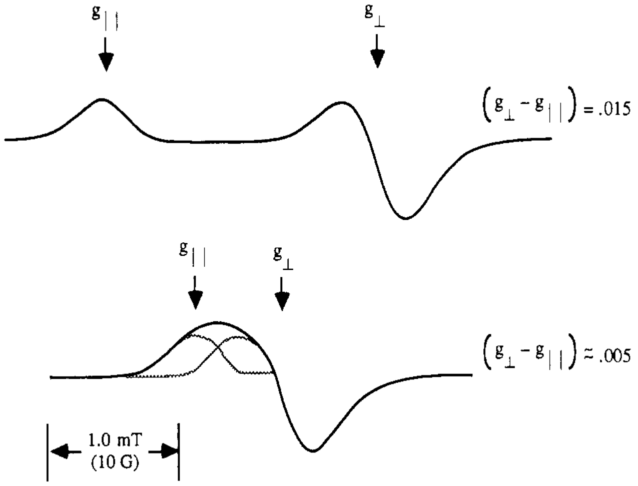

Figure 7. Line shapes expected for a g anisotropy of (a) $(g_\perp - g_\parallel) = 0.015$ and (b) $(g_\perp - g_\parallel) = 0.005$.

The line-shape parameters A/B and ΔH used to describe the line-shape changes are defined in Figure 3. As also shown, $\langle g \rangle$, the effective g value is defined as $\langle g \rangle = h\nu/\beta H_0$ where ν is the microwave frequency, β is the Bohr magneton, h is Planck's constant, and H_0 is the magnetic field value at which the first derivative crosses the base line. At all iodine concentrations, only one ESR line is resolved. However, to account for the changes in $\langle g \rangle$ and the line-shape parameters with iodine content, we consider the spectrum observed at any given iodine concentration to be a superposition of the ESR spectra from all the polaron species and all the ionized bipolaron species at that concentration. Iodine is diamagnetic in the form I_3^- but paramagnetic in the form I_2^-. In the latter case, the large anisotropy to be expected will broaden the ESR line beyond detection.[8] Hence, although no ESR line other than that described was observed, it is still possible that some I_2^- is present in the samples. With the large amounts of iodine present, this I_2^- might be detectable from measurements of the static magnetic susceptibility.

The value of $\langle g \rangle$ depends on the principal values of the **g** tensor averaged over all orientations. As can be seen in Figure 4, as the iodine concentration is increased from 0 to ~100 wt %, $\langle g \rangle$ increases monotonically. This behavior can be explained in terms of the equilibria scheme shown in Figure 2. The radical species with the higher iodine contents should show larger $\langle g \rangle$ values because of the increased spin–orbit interaction with a greater number of iodine atoms. Furthermore, as the iodine concentration is increased, the equilibria move to the right and also vertically downward. The gradual increase in $\langle g \rangle$ with increasing iodine content is therefore a result of increasing amounts of the species with the higher iodine stoichiometries. The decrease in $\langle g \rangle$ value with decreasing iodine concentration observed on the first removal of iodine is a result of the equilibria in Figure 2 reverting up and to the left and hence to an increase in the relative amounts of radical species with the lower stoichiometric amounts of iodine.

The values of A/B and ΔH are determined by g anisotropy, the homogeneous packet width, and possibly the unresolved proton hyperfine interactions. Figure 7 depicts the typical line shapes that can be expected by assuming an axial **g** tensor with the g anisotropy $(g_\perp - g_\parallel) = 0.015$ and $(g_\perp - g_\parallel) = 0.005$. We therefore attribute the asymmetry $(A/B \neq 1)$ in the observed spectra to g anisotropy. Hence, the initial monotonic increase of A/B and ΔH with increasing iodine content, shown in Figures 5 and 6, can also be explained in terms of an increase in the relative number of radical species with the higher iodine stoichiometries and larger spin–orbit coupling. The decrease in A/B and ΔH with increasing iodine concentration above 50 wt % iodine content may be the result of the ionized bipolaron having less g anisotropy than the polaron.[9] There may also be some reduction in A/B because of spin exchange.

As shown in Figures 4–6, at any given iodine concentration the values of $\langle g \rangle$, A/B, and ΔH measured on the first removal, second addition, and second removal of the iodine indicates that after the initial high doping the $\langle g \rangle$ values and line-shape parameters are reversible. However, the data also show that the values obtained on the first addition and first removal are different presumably because (as shown in Figure 1) the radical concentrations are different.[10]

On removal of the iodine, the A/B values decrease with decreasing iodine content such that below 50 wt % the ESR line is almost symmetrical. In this region the line shape is neither pure Gaussian nor pure Lorentzian, but somewhere in between. As shown in Figures 1 and 6, over the same range of iodine concentration, both the radical concentration and ΔH first decrease with decreasing iodine content, and then below 50 wt % iodine, both increase again. If we assume, for the reasons given above, that the ionized bipolaron has less g anisotropy than the polaron, then we can expect an increase in the g anisotropy with decreasing iodine content down to 50 wt % iodine. Moreover, below this iodine concentration, we can expect the g anisotropy to decrease because increased amounts of the species with lower iodine stoichiometries are indicated by the equilibria scheme in Figure 2. This implies that both A/B and ΔH should first increase and then decrease with decreasing iodine content. We suggest that intermolecular spin–spin interactions explain the deviations from this behavior and the differences between the values of A/B and ΔH measured in the first doping stages and those measured in the later stages.

As shown in Figure 1, the radical concentrations are much higher in the stages of the doping cycle after the first complete addition of iodine. These higher radical concentrations mean that intermolecular dipolar and exchange effects have to be considered in any analysis of the line-shape behavior. The dipolar interactions have a r_{ij}^{-3} dependence where r_{ij} is the distance between the ith and jth electron spin, whereas the exchange interaction is of the form $-\mathbf{J}\mathbf{S}_i\cdot\mathbf{S}_j$ where $\mathbf{J}$ is the intermolecular exchange integral that depends on the overlap between the spatial parts of the wave function for the ith and jth unpaired electron.

With our limited knowledge of the spin system, it is not possible to obtain a detailed understanding of how intermolecular dipolar and exchange interactions affect the line-shape parameters. However, we can expect the following qualitative effects. As the dipolar interactions are increased, the line width of the homogeneous spin packet width increases. Even with inhomogeneous broadening present, as a result of dipolar interactions the overall width should always increase with increasing radical concentration. On the other hand, spin exchange produces effects on the line shape that are similar to those caused by molecular reorientational motions since the intermolecular exchange modulates the g anisotropy, as well as the dipolar and hyperfine interactions.[11] Thus, increasing the exchange frequency ($\omega_e = 2J/\hbar$) by increasing the radical concentration first causes dynamic line shifts and line broadenings of the homogeneous spin packet widths. At high exchange frequencies (i.e., when $\omega_e \gg D/\hbar$ where D is the dipolar constant) where only one line remains in the spectrum , this line will undergo narrowing.

We can anticipate that as the exchange frequency increases $\langle g \rangle$ and the g anisotropy are reduced so that $\langle g \rangle$ tends toward its isotropic value and A/B decreases. The behavior of ΔH with exchange frequency depends on how it arises. Thus, if ΔH is determined primarily by the g anisotropy, as is shown in Figure 7, ΔH appears like a splitting and will decrease with increasing exchange frequency. On the other hand, if ΔH is determined by the spin packet width (i.e., the dipolar spin–spin interactions), in the slow-exchange region ΔH will increase with increasing exchange frequency. Thus, the data in Figure 6 for the first removal and second addition of iodine which shows that ΔH increases with radical concentration can be understood in terms of the latter process, viz., slow exchange.

The maximum radical concentration, shown in Figure 1 at an iodine content of 17 wt %, was found to be 1.0×10^{19} spins/g. In a polymer with a density of 1 g/cm^3, this radical concentration implies an average separation of $\sim$5 nm between electron spins; alternatively, with a molecular weight of 865 g/mol, this is equivalent to one polaron per 70 oligomers. If the polaron is at a fixed site in the oligomer and its wave function is restricted to 12 carbon atom sites, a distance of 5 nm is too great for there to be much orbital overlap. However, the exchange interactions can be greater than those estimated from the radical concentrations for the following reasons: (1) The average distance between polarons could be less than 5 nm because of clustering. This nonuniform distribution would occur if the iodine penetrated only to a certain depth from the surface of the powder particles because of slow diffusion rates. (2) Delocalization of the polaron over the oligomer chain (56 carbon sites) would increase the exchange interaction. (3) Fast translational motion of the polaron down the oligomer chain and from chain to chain would increase the exchange interactions. There is no definite evidence from the ESR data that such fast motion is present; indeed, the lack of such motion could explain the low electrical conductivity.

Conclusions

We have interpreted the dependence of the spin susceptibility of a conjugated oligomer on the iodine content in terms of the formation of polarons, bipolarons, and ionized bipolarons. Some of the gradual changes in the values of $\langle g \rangle$, A/B, and ΔH observed on varying the iodine content can be understood in terms of an equilibria scheme involving different stoichiometric forms of the paramagnetic polarons and the ionized bipolarons. Furthermore, at many iodine contents the radical concentrations are high enough that the behaviors of the line-shape parameters are complicated by intermolecular spin–spin interactions.

Acknowledgment. This work was supported by the McDonnell Douglas Independent Research and Development Program and the Dayco Corp. We are grateful to D. P. Ames and S. I. Weissman for their comments and suggestions on reading the manuscript.

Registry No. (4,4′-Dibromobiphenyl)(1,4-diethynylbenzene) (copolymer), 114490-31-2.

References and Notes

(1) Etemad, S.; Heeger, A. J.; MacDiarmid, A. G. *Annu. Rev. Phys. Chem.* **1982**, *33*, 443.
(2) Skotheim, T. A., Ed. *Handbook of Conducting Polymers*; Marcel Dekker: New York, 1986; Vols. I and II.
(3) Scott, J. C.; Pfluger, P.; Krounbi, M.; Street, G. B. *Phys. Rev.*

B: *Condens. Matter* **1983**, *28*, 2140.
(4) Bredas, J. L.; Chance, R. R.; Silbey, R. *Phys. Rev. B*: *Condens. Matter* **1982**, *26*, 5843.
(5) The maximum conductivity measured in these samples was 8 × 10^{-6} Ω^{-1} cm^{-1} at an iodine content of 26 wt %; the conductivity in the undoped sample was $<10^{-12}$ Ω^{-1} cm^{-1}.
(6) Sanechika, K.; Yamamoto, T.; Yamamoto, A. *Bull. Chem. Soc. Jpn.* **1984**, *57*, 752.
(7) Trumbo, D. L.; Marvel, C. S. *J. Polym. Sci., Polym. Chem. Ed.* **1986**, *24*, 2311.
(8) Boesman, E.; Schoemaker, D. *J. Chem. Phys.* **1962**, *37*, 671.
(9) We are unaware of any evidence reported in the literature to support this idea of reduced *g* anisotropy in an ionized bipolaron.
(10) The values for the spin susceptibility, ⟨*g*⟩, and line-shape parameters obtained on the first addition of iodine depend only on the iodine content. No time dependence was observed in samples kept at room temperature if the iodine content was constant.
(11) Kubo, R.; Tomita, K. *J. Phys. Soc. Jpn.* **1954**, *9*, 888.

Dynamics of Adsorbed Polymers. 1. Thickness Relaxation of Poly(vinylpyrrolidone) on Glass

Martinus A. Cohen Stuart[*] and Hisashi Tamai[†]

Laboratory for Physical and Colloid Chemistry, De Dreijen 6, 6703 BC Wageningen, The Netherlands, and Department of Applied Chemistry, Faculty of Engineering, Hiroshima University, Shitami Saijō-chō, Higashihiroshima-city, 724 Japan.

Received June 17, 1987; Revised Manuscript Received October 23, 1987

ABSTRACT: We present kinetic data that give a rather direct insight into the time scale of rearrangement processes occurring inside an adsorbed polymer layer. In particular, we were able to measure the hydrodynamic thickness of a freshly deposited adsorption layer as a function of time, and we found it to decrease over a time of the order of minutes. We present data for this relaxation process, which show that it is not simply exponential and that it strongly depends on the thickness increment prior to relaxation. We also present data on the relaxed thickness as a function of the number of deposition steps, polymer concentration, and molecular weight. The results can be qualitatively understood in terms of a simple two-stage adsorption.

Introduction

Static properties of adsorbed polymers have received much attention over more than 2 decades. As a result of numerous efforts there is now a considerable body of detailed knowledge, both theoretical and experimental. The state of the art has been discussed in recent reviews.[1,2]

Dynamic properties, on the other hand, are largely unknown. In some cases, a measured property, e.g., adsorbed amount or surface pressure, has been reported as a function of time,[3-5] but the number of systematic studies is small. Some careful kinetic studies were carried out in Strassbourg, both on the overall kinetics[6,7] and on the kinetics of exchange between adsorbed and free molecules in a saturated adsorption layer.[8] Rheological properties of polymers at fluid interfaces have been studied,[9] and it has been proposed that such layers may have glasslike properties under suitable conditions.[10,11] A kinetic theory for exchange with a saturated layer was proposed.[12]

A very characteristic aspect of polymer adsorption is the change in conformation that molecules must undergo to minimize the free energy. Since the rearrangement processes that must lead to equilibrium conformations are an essential aspect of the adsorption process, it would be interesting to have some information on the time scales involved. However, such information cannot easily be extracted from studies published so far, since these studies dealt with situations where the adsorbent surface was continuously in contact with a polymer solution of finite concentration. Under such conditions, transport by diffusion and conformational rearrangement occur simultaneously, and the two processes can be separated only with the help of a theoretical model. Such approaches provide, at best, circumstantial evidence.

Table I
PVP Polymer Samples

sample	$10^3[\eta]$, dm^3 g^{-1}	M_w, g mol^{-1}
K-17	7.8	8900
K-30	22.2	43000
K-30_{III}	40.5	102000
K-90	160.4	731000
K-90_{III}	76.5	254000

We therefore took a different approach. First of all, we decided to study the hydrodynamic thickness of adsorption layers during their formation, since from earlier work[13,14] we expected this quantity to the rather sensitive to conformational rearrangement. A polymer molecule that just starts to adsorb is still dilute and would stick out far into the solution, thus contributing strongly to the hydrodynamic thickness. As the chain is gradually pulled inward, we expect the thickness to decrease. In earlier work, we have shown that for uncharged polymers adsorbing from aqueous solution, the hydrodynamic layer thickness can be accurately measured by means of electrokinetic (preferably streaming potential) measurements at low ionic strength, especially if the layer thickness is not too large.[13] We therefore adopted this technique.

Second, we decided to study the rearrangement process in isolation, by suppressing polymer transport from the solution to the interface. This calls for an instantaneous removal of free molecules from the system. In our setup the adsorption occurs at the inner wall of a capillary that is continuously flushed with an aqueous electrolyte solution. Jumps between zero and finite polymer concentration can be easily achieved by pulsewise injection of polymer solution into the flowing electrolyte.

Experimental Section

Materials. Commercially available poly(vinylpyrrolidone) (PVP, Kollidon from BASF) was used. Three rather polydisperse samples (K-17, K-30, and K-90) of different molecular weight and

---

[*] To whom correspondence should be addressed at the Laboratory for Physical and Colloid Chemistry.
[†] Hiroshima University.